

**A novel transgenic mouse model of the human multiple myeloma
chromosomal translocation t(14;16)(q32;q23).**

Authors: Naoki Morito ¹, Keigyou Yoh ¹, Atsuko Maeda ², Takako Nakano ², Akiko
Fujita ¹, Manabu Kusakabe ², Michito Hamada ², Takashi Kudo ², Kunihiro Yamagata ¹
and Satoru Takahashi ²

Affiliations: ¹ Department of Nephrology, Doctoral Program in Clinical Sciences,

² Department of Anatomy and Embryology, Life System Medical Sciences,

Graduate School of Comprehensive Human Sciences, University of Tsukuba, 1-1-1 Tennodai,

Tsukuba, Ibaraki, 305-8575, Japan

Corresponding author; Satoru Takahashi, M.D., Ph. D.,

Department of Anatomy and Embryology, Life System Medical Sciences, Graduate School of
Comprehensive Human Sciences, University of Tsukuba, 1-1-1 Tennodai, Tsukuba 305 8577,
Japan.

e-mail: satoruta@md.tsukuba.ac.jp Tel no.: 81-29-853-7516; Fax no.: 81-29-853-6965

Words counts; Abstract (142 words) and the body of the manuscript (4979 words).

Running Title: Mouse model of the t(14;16)(q32;q23) translocation.

PRECIS: A novel transgenic mouse model may offer an ideal system to study the
pathogenesis of human multiple myeloma, an aggressive disease that remains relatively
poorly managed.

Abstract

Multiple myeloma (MM) is a currently incurable neoplasm of terminally-differentiated B cells. The translocation and/or overexpression of *c-MAF* have been observed in human MM. Although *c-MAF* might function as an oncogene in human MM, there has been no report thus far describing the direct induction of MM by *c-MAF* overexpression *in vivo*. In this study, we have generated transgenic mice that express *c-Maf* specifically in the B cell compartment. Aged *c-Maf* transgenic mice developed B cell lymphomas with some clinical features that resembled those of MM, namely plasma cell expansion and hyperglobulinemia. Quantitative RT-PCR analysis demonstrated that *Ccnd2* and *Itgb7*, which are known target genes of c-Maf, were highly expressed in the lymphoma cells. This novel transgenic mouse model of the human MM t(14;16)(q32;q23) chromosomal translocation should serve to provide new insight into the role of *c-MAF* in tumorigenesis.

Introduction

Multiple myeloma (MM) is an incurable neoplasm of terminally-differentiated B cells that is characterized by monoclonal expansion of malignant plasma cells. The common premalignant stage of MM is a monoclonal gammopathy of undetermined significance (MGUS), which progresses to MM at the rate of 1% of patients per year (1). Extensive genomic analysis has revealed that approximately 50% of patients with MGUS and MM have primary translocations in the clonal plasma cells that involve the immunoglobulin heavy chain (*IGH*) locus on chromosome 14q32 (2). Chromosomal translocations that involve the juxtaposition of the *IGH* locus with the loci for *CYCLIN D1* (3), *FGFR3* (4), or *MMSET* (5) result in the overexpression of these genes. It was first reported a decade ago that c-MAF is expressed at high levels in MM cells that carry the translocation t(14;16)(q32;q23), in which the *IGH* locus is fused with the *c-MAF* gene locus (6). In addition, c-MAF is overexpressed in 50% of MM cell lines and patients (7).

The *maf* proto-oncogene was identified originally within the genome of the avian musculoaponeurotic fibrosarcoma virus, AS42 (8). The product of the *Maf* gene and other members of the Maf family share a conserved basic-region leucine zipper (bZIP) motif that mediates dimer formation and DNA binding to the Maf recognition element (MARE) (9). Large Maf proteins, such as c-Maf, Mafk, Mafk/L-Maf/SMaf and Nrl, also contain an acidic domain that mediates transcriptional activation and plays a

key role in cellular differentiation (8-12). *c-Maf* encodes a T helper cell type 2 (Th2)-specific transcription factor that activates the expression of interleukin (IL)-4 in T cells (13). c-Maf is also involved in the regulation of lens fiber cell differentiation (14-16). Recently, we have found that transgenic mice that express c-Maf specifically in the T-cell compartment develop T-cell lymphoma (17). Furthermore, 60% of human T-cell lymphomas, classified as angioimmunoblastic T-cell lymphomas, were found to overexpress c-MAF (17, 18).

On the basis of the above facts, we hypothesized that overexpression of *c-Maf* in the B cell lineage would enhance the development of an MM-like disease. In this study, we have generated *c-Maf* transgenic mice that overexpress c-Maf in the B-cell compartment, using the *IgH* promoter and *E μ* enhancer. We found that these mice developed B cell lymphoma, which provided the first direct evidence that *c-Maf* can function as an oncogene in a murine model of the t(14;16)(q32;q23) translocation.

Materials and Methods

Mice. We made two constructs for the *Eμ c-Maf* transgene (Fig. 1A). For construct-1, we used the *Eμ* enhancer and the *V_H* promoter, as described previously (19). A 1.5-kb full-length cDNA that encoded the murine c-Maf protein was inserted into a vector that contained the *V_H* promoter and *Eμ* enhancer. Construct-1 was injected into fertilized eggs from BDF1 mice to generate transgenic mice, and then backcrossed four times into C57BL/6J. For construct-2, the *V_H* promoter, *Eμ* enhancer, and 3'*Eκ* enhancer were used. Construct-2 was injected into fertilized eggs from C57BL/6J mice to generate transgenic mice. Mice were maintained with a C57BL/6J genetic background in specific pathogen-free conditions in a Laboratory Animal Resource Center. All experiments were carried out according to the Guide for the Care and Use of Laboratory Animals at the University of Tsukuba.

Southern hybridization analysis. High molecular weight DNA was prepared from the tail of each mouse, and 10 μg of this DNA was digested with *EcoR* I and *Hind* III, and then Southern hybridization was performed, as described previously (17). To investigate *IgH* gene rearrangement, DNA from the tail and other tissues was examined by Southern hybridization. DNA that had been digested with *EcoR* I was hybridized with the *JH4* fragment, as described previously (20).

Isolation of mouse B220⁺ cells and RT-PCR to analyze transgene expression.

B220⁺ splenic B cells were isolated using magnetic microbeads from Miltenyi Biotec (Gladbach, Germany). Total RNA was prepared from the B220⁺ splenic B cells of 10 weeks old transgenic mice or their *wild-type* littermates using TRIzol reagent according to the manufacturer's instructions (Invitrogen, Carlsbad, CA). Total RNA (1 μ g) was reverse transcribed into cDNA using SuperScript III Reverse Transcriptase (Invitrogen), and 1 μ l of this 20 μ l reaction mixture was used for PCR. The *c-Maf* sequence was amplified using the primers 5'-CCTGCCGCTTCAAGAGGGTGC-3' and 5'-TCGCGTGTCACTCACATG-3', which yielded a 225-bp product. The sequence of *hprt* (hypoxanthine guanine phosphoribosyl transferase), which was used as a control, was amplified using the primers 5'-CAAACCTTTGCTTTCCTGGT-3' and 5'-CAAGGGCATATCCAACAACA-3', which yielded a 250-bp product.

Western blot analysis. Nuclear extracts were prepared from the B220⁺ splenic B cells of 10 weeks old transgenic or *wild-type* mice. The extracts were fractionated by size on a 10% SDS-polyacrylamide gel, transferred to a polyvinylidene difluoride membrane (Fluoro Trans; Pall BioSupport Division, Port Washington, NY), and incubated with primary and secondary antibodies. To detect the c-Maf protein, a rabbit antibody against mouse c-Maf was used as the primary antibody and peroxidase-conjugated goat anti-rabbit IgG (Zymed Laboratories, San Francisco, CA)

was used as the secondary antibody. The anti-c-Maf antibody was kindly provided by Dr. Masaharu Sakai (University of Hokkaido, Sapporo, Japan). To normalize the results with respect to the amount of protein in each sample, a goat antibody against mouse Lamin B (Santa Cruz Biochemicals, Santa Cruz, CA) was used.

Flow cytometry analysis. Single-cell suspensions were prepared from the spleen and the bone marrow of each mouse. Multicolor flow cytometric analysis was performed using an LSR Flow Cytometer and CellQuest software (Becton Dickinson, Franklin Lakes, NJ). The PE-labeled rat antibodies against mouse CD3, CD138, CD23 and IgD, the FITC-labeled rat antibodies against mouse B220, CD21 and IgM, and APC-labeled rat antibody against mouse B220 were obtained from BD Pharmingen (San Diego, CA).

Cell culture of B cells. B220⁺ cells (2×10^5) were plated in triplicate on 96-well plates before stimulation with lipopolysaccharide (LPS; 10 µg/ml; Sigma) and anti-mouse CD40 (1 µg/ml; BD Pharmingen). After 16 hr of stimulation, the viable cell number was determined using a CellTiter 96 Aqueous One Solution Cell Proliferation Assay (Promega, Madison, WI). Aliquots of 40 µl of CellTiter 96[®] Aqueous One Solution were added to each well and incubated for an additional 3 hrs before the final absorbance at 490 nm was determined.

Measurement of serum immunoglobulins, paraprotein determination and X-Ray

analysis. The amounts of IgG, IgM, and IgA were determined by ELISA, as described previously (21). Paraproteins (M spikes, extra gradients) were determined by SRL, Inc. (Tokyo, Japan). X-ray analysis of bones was performed using a Faxitron X-ray Specimen Radiographic System (Lincolnshire, IL) and Kodak X-OMAT-TL film (Rochester, NY).

Histopathologic analysis. Each mouse was bled under ether anesthesia. At autopsy, organs were fixed with 10% formalin in 0.01 M phosphate buffer (pH 7.2) and embedded in paraffin. Sections were stained with Hematoxylin and Eosin (H&E) and Periodic acid-Schiff (PAS) stain for histopathologic examination by light microscopy. For dual immunofluorescent staining, the rabbit antibody against mouse c-Maf, FITC-labeled goat anti-rabbit IgG (green), and PE-labeled rat anti-mouse CD138 antibody (red) were used. The anti-CD138 and anti-B220 antibodies were purchased from BD Pharmingen. The immunohistochemical analysis of CD138 and anti-B220 were performed by the avidin-biotin-peroxidase complex staining technique. For immunofluorescent analysis, frozen sections were stained with FITC-labeled goat antibodies against mouse immunoglobulins IgG, IgM, IgA, kappa light chain, and lambda light chain (ICN Pharmaceuticals, Cleveland, OH).

Quantitative reverse transcription-PCR. Total RNA (1 μ g) was reverse transcribed into cDNA. Each reaction was done in duplicate. The quantity of cDNA in each sample was normalized to the amount of *hprt* cDNA. For the PCR, we used SYBR[®] Premix Ex Taq[™] II (TAKARA Bio, Shiga, Japan) according to the manufacturer's instructions. The amplification was carried out in a Thermal Cycler Dice[®] Real Time System (TAKARA Bio). The following primer pairs were used: *c-Maf* forward: 5'-CTGCCGCTTCAAGAGGGTGCAGC-3' and *c-Maf* reverse: 5'-GATCTCCTGCTTGAGGTGGTC-3'; *Cyclin D2* forward: 5'-CCTCTTCTTCACACTTTTGTGGTC-3' and *Cyclin D2* reverse: 5'-CTACCTCCCGCAGTGTTCCCT-3'; *Integrin β 7* forward: 5'-CAACCTGGACTCACCCGAAG-3' and *Integrin β 7* reverse: 5'-CTACCTCCCGCAGTGTTCCCT-3'; *Prdm1* forward: 5'-AAGCCGAGGCATCCTTACC-3' and *Prdm1* reverse: 5'-GTCCAAAGCGTGTTCCCTTC-3'; *Pax5* forward: 5'-ACAAACGCCAAAACCCTACC-3' and *Pax5* reverse: 5'-CTGCTGTACTTTTGTCCGAATGA-3'; *Xbp1* forward: 5'-GGAGCAGCAAGTGGTGGATT-3' and *Xbp1* reverse: 5'-CAGCGTGTCCATTCCCAAG-3'; *c-Myc* forward: 5'-GATTCCTTTGGGCGTTGG-3' and *c-Myc* reverse: 5'-GAGGTCATAGTTCCTGTTGGTGAAG-3'; *Irf4* forward:

| | | | |
|---------------------------------|-----|-------------|----------|
| 5'-GGTGTACAGGATTGTTCCAGAGG-3' | and | <i>Irf4</i> | reverse: |
| 5'-GCAGAGAGCCATAAGGTGCTG-3'; | | <i>Spp1</i> | forward: |
| 5'-GCTTGGCTTATGGACTGAGGT-3' | and | <i>Spp1</i> | reverse: |
| 5'-TCAGAAGCTGGGCAACAGG-3'; | | <i>Hprt</i> | forward: |
| 5'-TTGTTGTTGGATATGCCCTTGACTA-3' | and | <i>Hprt</i> | reverse: |
| 5'-AGGCAGATGGCCACAGGACTA-3'. | | | |

Statistical analysis. Results were expressed as the mean \pm SE. Data were compared by one-way analysis of variance (ANOVA) and the Bonferroni correction was applied routinely. Significant differences between the groups of mice were analyzed using the Wilcoxon test for paired samples, and values of $p < 0.05$ were considered statistically significant. Survival rates were compared using the Kaplan-Meier method.

Results

Generation of E μ c-Maf transgenic mice that express c-Maf specifically in B cells. To generate transgenic mice that express high levels of c-Maf specifically in B cells, the murine *c-Maf* coding sequence was inserted into a vector that contained the *V_H* gene promoter, an *E μ* enhancer sequence, and a 3' *E κ* enhancer sequence (Fig. 1A). We generated two constructs (the first did not contain the 3' *E κ* enhancer) and obtained 17 F0 transgenic mice with a BDF1 or C57BL/6J genetic background. Subsequently, three transgenic mouse lines with a C57BL/6J genetic background were generated, and screened by PCR using tail DNA as the template. Genomic DNA was analyzed by Southern blotting to confirm the integrity and copy number of the transgene in each transgenic line. The *Eco*R I/ *Hind* III fragment that contained the *c-Maf* transgene was 1.3 kb in length, whereas the corresponding fragment for the endogenous *c-Maf* gene was 4.0 kb. The results of densitometric analyses revealed that TG (transgenic) line 524, which was generated using construct-1, contained approximately four copies of the transgene, whereas TG lines 99 and 68, which were generated with construct-2, both contained approximately two copies (Fig. 1B, a). These transgenes were stably transmitted to the progeny.

Overexpression of *c-Maf* in transgenic mice. To confirm that the transgene was expressed, the levels of *c-Maf* mRNA and protein in splenic B cells from the TG lines were monitored by RT-PCR and western blotting (Fig. 1B, b and c). The *c-Maf* mRNA was overexpressed in all the transgenic mice that were tested (Fig. 1B, b). Correspondingly, western blot analysis of B220⁺ splenic B cells confirmed that the levels of c-Maf protein were elevated (Fig. 1B, c). c-Maf protein was not detected in *wild-type* B cells in this analysis.

B cell development and proliferative potential in *Eμ c-Maf* transgenic mice. To investigate the effect of c-Maf overexpression on B-cell differentiation, we carried out flow cytometric analysis of splenocytes isolated from transgenic mice at 20 weeks of age. Flow cytometry showed that the total numbers of T cells (CD3⁺) and B cells (B220⁺) in the spleens of *Eμ c-Maf* transgenic mice were unaltered relative to *wild-type* mice (Fig. 1C). In addition, we could not find any apparent differences in the subpopulations of B cells, namely follicular cells (B220⁺ CD23^{high} CD21⁻) and marginal zone (MZ) B cells (B220⁺ CD23⁻ CD21^{high}) (Fig. 1C). Next, we analyzed the proliferative potential of *wild-type* and *Eμ c-Maf* transgenic B cells *in vitro*. The proliferative potential of *Eμ c-Maf* transgenic B cells was relatively high, but there was no substantial difference in the response to LPS (Fig. 1D) or CD40 (data not shown) between the two groups.

Aged $E\mu$ c-Maf transgenic mice developed lymphoma. The *E μ c-Maf* transgenic mice appeared healthy up to 50 weeks of age. However, they subsequently developed tumors. The mean age at diagnosis as lymphoma by histological analysis was 80.1 weeks. We confirmed that 28% (18/64) of the *E μ c-Maf* transgenic mice developed lymphoma (Fig. 2A). We could not detect any apparent difference in survival between the mice that were generated with the two different constructs, construct-1 for TG524, and construct-2 for TG 99 and 68.

Lymphomas observed in $E\mu$ c-Maf transgenic mice were of B-cell origin. *E μ c-Maf* transgenic mice appeared healthy up to 50 weeks of age, but they developed tumors subsequently. We performed histological analysis to identify the origin of the lymphoma cells. The spleens of the *E μ c-Maf* transgenic mice were enlarged approximately two- to five-fold relative to those of the *wild-type* mice. The spleens of the mice with lymphoma were infiltrated by numerous cells, which partially destroyed the normal tissue architecture (Fig. 2B). Cells that had infiltrated demonstrated plasma cell-like morphology (Fig. 2B). Moreover, immunohistochemical analysis revealed that the infiltrating cells were B220⁺ (Fig. 2C), and also expressed CD138 (Fig. 2C). We confirmed that the infiltrating cells were positive for both CD138 and c-Maf by immunofluorescence staining (Fig. 2C). To investigate the characteristics of

the lymphoma cells, we performed flow cytometry (Fig. 2C and D). We found the number of B220⁺ CD138⁺ CD21⁺ CD23⁺ IgM⁺ IgD⁻ cells was increased in the transgenic mice relative to the *wild-type* mice. We also found that the number of mature plasma cells (B220^{low} CD138⁺) was increased in the transgenic mice (Fig. 2C).

Hypergammaglobulinemia in aged Eμ c-Maf transgenic mice. Approximately 50% (7/14) of the *Eμ c-Maf* transgenic mice of line 524 showed a clonal M spike in the serum between 20 and 50 weeks of age (Fig. 3A). At 120 weeks old, 35% (5/14) of these transgenic mice had developed lymphoma. The remaining mice that showed a clonal M spike (2/14) demonstrated no evidence of lymphoma at 120 weeks. The plasma levels of both IgG and IgM, as measured by ELISA, were increased significantly in aged *Eμ c-Maf* transgenic mice (Fig. 3B). The mean amount of total IgG in the transgenic mice was 1760 ± 302 (mg/dl), whereas in the control mice this value was 934 ± 142 (mg/dl) ($p < 0.05$). In addition, the mean amount of total IgM in the transgenic mice was 1083 ± 223 (mg/dl), whereas in the control mice this value was 564 ± 92 (mg/dl). However, there was no obvious elevation of total IgA in the transgenic mice. It must be noted that only one out of the 14 mice showed high levels of both IgG and IgM (Fig. 3B). Notably, these changes in the serum were associated with increased numbers of mature plasma cells (B220^{low} CD138⁺) in the bone marrow; the proportion of plasma cells as a percentage of the total number of bone marrow

cells was 5–20% in the transgenic mice compared to <5% in the non-transgenic controls (Fig. 3C). We also found the number of B220⁺ CD138⁺ cells in the bone marrow was increased (Fig. 3C). However, we could not identify any obvious osteolytic lesions by X-ray analysis (Fig. 3C).

Eμ c-Maf transgenic mice showed clinical features that resembled those of patients with plasma cell disorders. In *Eμ c-Maf* transgenic mice with hyperglobulinemia that were over 60 weeks old, renal tubular casts and tubular obstruction were observed (Fig. 4A), which resembled human myeloma kidney (so-called cast nephropathy) (22). Moreover, glomerular changes that were characterized by mesangial widening due to the deposition of PAS-positive material were observed in aged *Eμ c-Maf* transgenic mice (Fig. 4A); this resembled monoclonal immunoglobulin deposition disease (MIDD) (22). These renal lesions were similar to the pathologic manifestations that are present in human MM and other plasma cell disorders in which the systemic chronic overproduction of immunoglobulins and the accumulation of light chains, paraproteins, and other immunoglobulin fragments are observed (22). The depositions contained immunoglobulin light and heavy chains, which consisted of either polyclonal heavy and light chains or clonal IgG or IgM heavy chains and kappa light chains (Fig. 4B).

Autonomous proliferation in nude mice of lymphoma cells from Eμ c-Maf transgenic mice. To ascertain whether the infiltrating tumor cells in *Eμ c-Maf* transgenic mice could proliferate autonomously, we isolated mononuclear cells from the spleens of these mice and injected the isolated cells into nude mice via the tail vein (10^6 cells/mouse). Recipient mice displayed prominent hepatomegaly, splenomegaly and/or enlarged lymph nodes throughout their bodies within 12 weeks of transplantation. A typical example is shown in Fig. 5A. The tumor cells could also be transplanted into syngeneic C57BL/6J mice. To assess clonality, we examined the rearrangement of the *IgH* locus in the *c-Maf* transgenic lymphoma cells. Southern blot analysis was carried out using a murine *JH4* probe (Fig. 5B). We extracted DNA from the tails, and spleens of the mice. Monoclonal rearrangement of the *IgH* locus was found in DNA that had been isolated from the spleens of the *Eμ c-Maf* transgenic mice (Fig. 5B, lanes 3 to 6). Histological analysis of the spleen from these recipient mice revealed that the tumor cells showed a plasma cell-like morphology, i.e. the same as the original lymphoma cells (Fig. 5C).

Expression of c-Maf target genes in Eμ c-Maf transgenic mice. To gain insight into the molecular mechanism by which plasma cell dyscrasia develops, we measured the level of mRNA expression from *c-Maf* and its target genes in *Eμ c-Maf* transgenic mice using a quantitative RT-PCR assay (Fig. 6). In human MM, *CYCLIN D2* and

INTEGRIN $\beta 7$ are known to be targets of c-MAF (7, 23). As we described previously, deregulated expression of *Cyclin D2* and *Integrin* $\beta 7$ is also observed in the T cell lymphomas of transgenic mice that overexpress c-Maf in the T lymphoid compartment (17). Therefore, we analyzed the expression of *Cyclin D2* and *Integrin* $\beta 7$ in *E μ c-Maf* transgenic mice. The level of *c-Maf* expression in the lymphoma-infiltrated lymph nodes of *E μ c-Maf* transgenic mice was three- to five-fold greater than the level in *wild-type* B cells (B220⁺) (Fig. 6). We confirmed the percentage of B220⁺ cells in the lymph nodes was over 70 %. We also found that the expression of both *Cyclin D2* and *Integrin* $\beta 7$ was elevated in *E μ c-Maf* transgenic mice (Fig. 6), which was consistent with the results of previous reports in human MM (7).

Next, we examined the levels of the B cell-associated transcription factors, *Prdm1* (Blimp-1), *Xbp1* and *Pax5*. Blimp-1 is a transcriptional repressor that plays a critical role in the terminal differentiation of B cells into antibody-secreting plasma cells (24). Overexpression of Blimp-1 has been shown to drive plasma cell differentiation (24-26). *Xbp1* is a basic-region leucine zipper (bZIP) transcription factor and a major regulator of plasma cell differentiation (27). It is known that *E μ Xbp1s* mice develop MM/MGUS (28). In addition, *Pax5* is known to inhibit plasmacytic development, and also to repress the expression of *Xbp1*, which is needed for plasma cell formation and immunoglobulin secretion (29). By RT-PCR analysis (Fig. 6), we found that *Prdm1* and *Xbp1* expression were increased, but *Pax5* expression was decreased, in the

transgenic mice as compared to the control mice, which might correlate with the plasma cell differentiation.

It is known that the dysregulation of MYC (c-MYC) expression can induce the progression of MGUS to MM (1). In addition, it has been reported that myeloma cells are completely dependent on the transcription factor IRF4 (interferon regulatory factor 4), despite that fact that most myeloma cells do not harbour mutations, translocations or amplifications of the *IRF4* locus (30). Moreover, IRF4 is itself a direct target of MYC, which generates an autoregulatory circuit in myeloma cells (30). However, neither *Myc* nor *Irf4* expression were elevated in the *Eμ c-Maf* transgenic mice. We also analyzed *Spp1* (osteopontin) expression, because we could not find any obvious osteolytic lesions in the *Eμ c-Maf* transgenic mice. *SPP1*, which is highly expressed in MM, plays a critical role in bone disease by protecting the bone from destruction (31). We observed that the expression of *Spp1* was up-regulated in *Eμ c-Maf* transgenic mice (Fig. 6).

Discussion

It is important to emphasize that *v-maf* is a classical oncogene that was identified in an avian transforming virus, AS42 (8). Large Maf proteins, such as c-Maf, Maf_b and Maf_a, can efficiently transform primary fibroblasts *in vitro* (9, 32-34). Previously, we generated *c-Maf* transgenic mice that overexpress *c-Maf* in the T-cell compartment using the VA vector, which contains the human CD2 promoter and locus control region. The VA *c-Maf* transgenic mice developed T-cell lymphoma, thus providing evidence that *c-Maf* can function as an oncogene in T cells *in vivo* (17). Work over the last decade has provided evidence that c-MAF might play crucial roles in the pathogenesis of MM. It has been reported that the translocation and/or overexpression of *c-MAF* are identified frequently in human MM (6, 7, 23). Translocations that involve *MAFA* (23, 35) or *MAFB* (t(14;20)(q32;q12)) (35, 36), which encode other large MAF proteins, have also been identified. Altogether, translocations that involve a large MAF transcription factor are found in 8–10% of MMs: *c-MAF* is translocated in 5%, *MAFB* in 2%, and *MAFA* in less than 1% of cases (23, 35). Although *c-MAF* translocations are observed in only 5–10% of MMs, *c-MAF* is overexpressed in 50% of cases (7, 23).

In this study, we demonstrated that aged *c-Maf* transgenic mice developed B cell lymphomas with some clinical features that resembled those of human MM, namely expansion of plasma cells, hyperglobulinemia, and renal involvement. Although we found that plasma cells (B220^{low} CD138⁺) were increased in the spleen and bone

marrow of the transgenic mice, the lymphoma cells in the spleens were B220⁺ CD138⁺ CD21⁺ CD23⁺ IgM⁺ IgD⁻. The phenotype of some *Eμ c-Maf* transgenic mice partially resembled that of types of B cell lymphoma that contain plasmablasts and/or plasma cells rather than plasma cell dyscrasias, such as Waldenström's macroglobulinemia (WM; also known as lymphoplasmacytic lymphoma) or MALT (mucosa associated lymphoid tissue) lymphoma. WM is classified as an indolent form of B-cell lymphoma. Infiltration with clonal lymphoplasmacytic cells, predominantly in the bone marrow, and an IgM monoclonal gammopathy are diagnostic findings of WM (37). MALT lymphoma is a distinct subtype of MZ B cell lymphomas. The large number of plasma cells among MALT lymphoma cells is a well known phenomenon known as plasmacytic differentiation (38). With the demonstration that the tumors express both mature B cell (B220⁺) and plasma cell (CD138⁺) markers, it should be noted that they fall within a spectrum of mouse plasma cell-related tumors (anaplastic, plasmablastic, and plasmacytic plasmacytoma) described, previously (39, 40, 41). The *Eμ c-Maf* transgenic mouse is a murine model of the human MM t(14;16)(q32;q23) chromosomal translocation. Primary early onset reciprocal chromosomal translocations in MM occur most frequently at *IGH* on 14q32. Meanwhile, secondary late onset translocations and gene mutations have been implicated in MM progression (42). The fact that *Eμ c-Maf* transgenic mice displayed immature phenotypes rather than classical MM might suggest that *c-MAF* translocation alone is not sufficient for

the development of classical MM. Experimental efforts to generate mouse models of MM have typically involved the targeted expression of an oncogene in the B cell compartment by transgenic approaches (28). These strategies have generally yielded B cell malignancies that display immature phenotypes or plasmacytomas rather than classical MM (28). Given that *c-MAF* is known to be translocated and/or overexpressed in human MM, the *E μ c-Maf* transgenic mouse may offer an ideal system to study the pathogenesis of human MM. Aged *E μ c-Maf* transgenic mice developed B cell lymphomas, rather than plasma cell dyscrasias. In the majority of cases, transgenic mice that express an oncogene or proto-oncogene specifically in the B cell compartment develop plasmacytoma, not classical MM. This is the case for *v-abl* (43), *Il-6* (44), and *Bcl-2/c-Myc* (45) mice; however, *E μ Xbp1s* (28) transgenic mice are the exception. Recently, it was reported that transgenic mice in which the *c-Myc* gene was subject to conditional Aid (Activation-Induced Deaminase)–dependent activation developed the MM/MGUS phenotype (46). We do not understand the underlying differences in the promotion of tumor formation between mice and humans.

Further studies will be needed to define the role of c-Maf in the development of both human and mouse MM. Clarification of the mechanism by which c-Maf contributes to oncogenesis may ultimately facilitate the discovery of more specific therapies to prevent the progression of MM.

Disclosure of Potential Conflicts of Interest

No potential conflicts of interest were disclosed

Grant Support

A Grant-in-Aid for Scientific Research on Priority Areas and Genome Network Project from the Ministry of Education, Culture, Sports, Science and Technology, Japan, a Grant-in-Aid for Exploratory Research (22650090), a grant from The Naito Foundation, and a grant from the Astellas Foundation for Research on Metabolic Disorders.

References

1. Kyle RA, Rajkumar SV. Multiple myeloma. *N Engl J Med* 2004;351:1860-73.
2. Sirohi B, Powles R. Epidemiology and outcomes research for MGUS, myeloma and amyloidosis. *Eur J Cancer* 2006;42:1671-83.
3. Chesi M, Bergsagel PL, Brents LA, et al. Dysregulation of cyclin D1 by translocation into an IgH gamma switch region in two multiple myeloma cell lines. *Blood* 1996;88:674-681.
4. Chesi M, Nardini E, Brents LA, et al. Frequent translocation t(4;14)(p16.3;q32.3) in multiple myeloma is associated with increased expression and activating mutations of fibroblast growth factor receptor 3. *Nat Genet* 1997;16:260-4.
5. Chesi M, Nardini E, Lim RS, et al. The t(4;14) translocation in myeloma dysregulates both FGFR3 and a novel gene, MMSET, resulting in IgH/MMSET hybrid transcripts. *Blood* 1998;92:3025-34.

6. Chesi M, Bergsagel PL, Shonukan OO, et al. Frequent dysregulation of the c-maf proto-oncogene at 16q23 by translocation to an Ig locus in multiple myeloma. *Blood* 1998;91:4457-63.
7. Hurt EM, Wiestner A, Rosenwald A, et al. Overexpression of c-maf is a frequent oncogenic event in multiple myeloma that promotes proliferation and pathological interactions with bone marrow stroma. *Cancer Cell* 2004;5:191-9.
8. Nishizawa M, Kataoka K, Goto N, et al. v-maf, a viral oncogene that encodes a "leucine zipper" motif. *Proc Natl Acad Sci USA* 1989;86:7711-5.
9. Kataoka K, Noda M, Nishizawa M, et al. Maf nuclear oncoprotein recognizes sequences related to an AP-1 site and form heterodimers with both Fos and Jun. *Mol Cell Biol* 1994;14:700-12.
10. Swaroop A, Xu J, Pawar H, et al. A conserved retina-specific gene encodes a basic motif/leucine zipper domain. *Proc Natl Acad Sci U S A* 1992;89:266-70.
11. Ogino H, Yasuda K, et al. Induction of lens differentiation by activation of a bZIP transcription factor, L-Maf. *Science* 1998;280:115-8.

12. Kajihara M, Kawauchi S, Kobayashi M, et al. Isolation, characterization, and expression analysis of zebrafish large Mafs. *J Biochem* 2001;129:139-46.
13. Ho IC, Hodge MR, Rooney JW, et al. The proto-oncogene c-maf is responsible for tissue-specific expression of interleukin-4. *Cell* 1996;85:973-83.
14. Kawauchi S, Takahashi S, Nakajima O, et al. Regulation of lens fiber cell differentiation by transcription factor c-Maf. *J Biol Chem* 1999;274:19254-60.
15. Kim JI, Li T, Ho IC, et al. Requirement for the c-Maf transcription factor in crystallin gene regulation and lens development. *Proc Natl Acad Sci U S A* 1999;96:3781–5.
16. Ring BZ, Cordes SP, Overbeek PA, et al. Regulation of mouse lens fiber cell development and differentiation by the Maf gene. *Development* 2000;127:307–17.
17. Morito N, Yoh K, Fujioka Y, et al. Overexpression of c-Maf contributes to T-cell lymphoma in both mice and human. *Cancer Res* 2006;66:812-9.

18. Murakami YI, Yatabe Y, Sakaguchi T, et al. c-Maf expression in angioimmunoblastic T-cell lymphoma. *Am J Surg Pathol* 2007;31:1695-702.
19. Nagaoka H, Takahashi Y, Hayashi R, et al. Ras mediates effector pathways responsible for pre-B cell survival, which is essential for the developmental progression to the late pre-B cell stage. *J Exp Med* 2000;192:171-82.
20. Costinean S, Zanesi N, Pekarsky Y, et al. Pre-B cell proliferation and lymphoblastic leukemia/high-grade lymphoma in E(mu)-miR155 transgenic mice. *Proc Natl Acad Sci USA* 2006;103:7024-9.
21. Morito N, Yoh K, Hirayama A, et al. Nrf2 deficiency improves autoimmune nephritis caused by the fas mutation lpr. *Kidney Int* 2004;65:1703-13.
22. Korbet SM, Schwartz MM. Multiple myeloma. *J Am Soc Nephrol* 2006;17:2533-45.
23. Eychène A, Rocques N, Pouponnot C. A new MAFia in cancer. *Nat Rev Cancer* 2008;8:683-93.

24. Turner CA Jr, Mack DH, Davis MM, et al. Blimp-1, a novel zinc finger-containing protein that can drive the maturation of B lymphocytes into immunoglobulin-secreting cells. *Cell* 1994;77:297-306.
25. Schliephake DE, Schimpl A. Blimp-1 overcomes the block in IgM secretion in lipopolysaccharide/ anti- μ F(ab')₂-co-stimulated B lymphocytes. *Eur J Immunol* 1996;26:268-71.
26. Piskurich JF, Lin KI, Lin Y, et al. BLIMP-1 mediates extinction of major histocompatibility class II transactivator expression in plasma cells. *Nat Immunol* 2000;1:526-32.
27. Reimold AM, Ponath PD, Li YS, et al. Transcription factor B cell lineage-specific activator protein regulates the gene for human X-box binding protein 1. *J Exp Med* 1996;183:393-401.
28. Carrasco DR, Sukhdeo K, Protopopova M, et al. The differentiation and stress response factor XBP-1 drives multiple myeloma pathogenesis. *Cancer Cell* 2007;11:349-60.

29. Reimold AM, Iwakoshi NN, Manis J, et al. Plasma cell differentiation requires the transcription factor XBP-1. *Nature* 2001;412:300-7.
30. Shaffer AL, Emre NC, Lamy L, et al. IRF4 addiction in multiple myeloma. *Nature* 2008;454:226-231.
31. Robbiani DF, Colon K, Ely S, et al. Osteopontin dysregulation and lytic bone lesions in multiple myeloma. *Hematol Oncol* 2007;25:16-20.
32. Kataoka K, Nishizawa M, Kawai S, et al. Structure-function analysis of the maf oncogene product, a member of the b-Zip protein family. *J. Virol* 1993;67:2133-41.
33. Nishizawa M, Kataoka K, Vogt PK, et al. MafA has strong cell transforming ability but is a weak transactivator. *Oncogene* 2003;22:7882-90.
34. Pouponnot C, Sii-Felice K, Hmitou I, et al. Cell context reveals a dual role for Maf in oncogenesis. *Oncogene* 2006;25:1299-310.

35. Chng WJ, Glebov O, Bergsagel PL, et al. Genetic events in the pathogenesis of multiple myeloma. *Best Pract Res Clin Haematol* 2007;20:571-96.
36. Hanamura I, Iida S, Akano Y, et al. Ectopic expression of MAFB gene in human myeloma cells carrying (14;20)(q32;q11) chromosomal translocations. *Jpn J Cancer Res* 2001;92:638-44.
37. Strasser A, Pascual V. Pathophysiology of Waldenström's macroglobulinemia. *Haematologica* 2010;95:359-64.
38. Cohen SM, Petryk M, Varma M, et al. Non-Hodgkin's lymphoma of mucosa-associated lymphoid tissue. *Oncologist* 2006;11:1100-17.
39. Qi CF, Zhou JX, Lee CH, et al. Anaplastic, plasmablastic, and plasmacytic plasmacytomas of mice: relationships to human plasma cell neoplasms and late-stage differentiation of normal B cells. *Cancer Res* 2007;67:2439-47.
40. Qi CF, Shin DM, Li Z, et al. Anaplastic plasmacytomas: relationships to normal memory B cells and plasma cell neoplasms of immunodeficient and autoimmune mice. *J Pathol* 2010; 221:106-16.

41. Ishikawa F, Saito Y, Shultz LD. Modeling Human Leukemia Using Immune-Compromised Mice. In: Li S, editor. Mouse Models of Human Blood Cancers. New York: Springer; 2008. p.121-9.
42. Raab MS, Podar K, Breitkreutz I, et al. Multiple myeloma. Lancet 2009;374:324-39.
43. Rosenbaum H, Harris AW, Bath ML, et al. An E mu-v-abl transgene elicits plasmacytomas in concert with an activated myc gene. EMBO J 1990;9:897-905.
44. Suematsu S, Matsusaka T, Matsuda T, et al. Generation of plasmacytomas with the chromosomal translocation t(12;15) in interleukin 6 transgenic mice. Proc Natl Acad Sci U S A 1992;89:232-5.
45. Stone MJ, Harris AW, Bath ML, et al. Novel primitive lymphoid tumours induced in transgenic mice by cooperation between myc and bcl-2. Nature 1990;348:331-3.

46. Chesi M, Robbiani DF, Sebag M, et al. AID-dependent activation of a MYC transgene induces multiple myeloma in a conditional mouse model of post-germinal center malignancies. *Cancer Cell* 2008;13:167-80.

Figure legends

Figure 1. Generation of mice that overexpress c-Maf. A, Constructs of the *Eμ c-Maf* transgene. The *c-Maf* cDNA was inserted into a vector that contained the *V_H* gene promoter (*Vp*), and an *Eμ* enhancer (*Eμ*), or one that contained *Vp*, *Eμ*, and a 3' *Eκ* enhancer (*Eκ*). The probe for Southern blot analysis, the restriction enzyme sites (*EcoR* I; E, and *Hind* III; H), and the predicted sizes of the endogenous gene and the transgene are indicated. Transgene construct-1 was used for TG line 524, whereas TG lines 99 and 68 were generated with construct-2. B-a, Southern blot analysis of the endogenous and transgenic *c-Maf* genes in *Eμ c-Maf* transgenic mice. The 4.0-kb endogenous and 1.3-kb transgenic gene fragments are shown for TG mice. B-b, Analysis of *c-Maf* mRNA in B cells. The amount of *c-Maf* mRNA in the samples from TG was higher than that in a sample from *wild-type* (WT) mice. B-c, Western blot analysis of splenic B220⁺ B cells from *Eμ c-Maf* transgenic mice (524, 99, and 68) and *wild-type* mice (WT). C, Immunofluorescence analysis of splenocyte subpopulations from *Eμ c-Maf* transgenic mice at 20 weeks of age. The total numbers of T cells (CD3⁺) and B cells (B220⁺) did not differ between the spleens of *wild-type* and *Eμ c-Maf* transgenic mice. There were no apparent differences in the subpopulations of B cells, namely follicular cells (B220⁺ CD23^{high} CD21⁻) and marginal zone (MZ) B cells (B220⁺ CD23⁻ CD21^{high}). D, Proliferative potential of B cells after treatment with LPS.

Enriched splenic B220⁺ cell populations obtained from *wild-type* and *Eμ c-Maf* transgenic mice at 20 weeks of age were cultured in the presence of LPS, and proliferation was assayed by using a CellTiter 96[®] Aqueous One Solution Cell Proliferation Assay. The mean absorbance at 490 nm is presented.

Figure 2. *Eμ c-Maf* transgenic mice developed B cell lymphoma. A, Cumulative lymphoma-free survival rate curves of *Eμ c-Maf* transgenic (TG) and *wild-type* (WT) mice. Statistically significant differences ($p<0.05$) were detected between the two groups. B, The number of plasma cell-like lymphoma cells in the spleens of *Eμ c-Maf* transgenic (TG) mice was increased compared to that in the controls (WT). Disruption of the normal follicles and accumulation of lymphoma cells were observed in spleens from the transgenic mice (H&E). C, The B cell lymphoma cells (B220⁺) also expressed CD138, as shown by immunohistochemical staining of B220 and CD138. Immunofluorescence showed that plasma cells (CD138⁺, red) that had infiltrated into the spleens of *Eμ c-Maf* transgenic mice also expressed c-Maf (green), but this was not observed in the spleens of *wild-type* mice. Flow cytometry revealed that the number of B220⁺ CD138⁺ cells was increased in the spleens of *Eμ c-Maf* transgenic mice that carried lymphoma. The number of mature plasma cells (B220^{low} CD138⁺) in the spleen was also increased. D, B220⁺ CD138⁺ cells in the spleens of *Eμ c-Maf*

transgenic mice were characterized as B220⁺ CD138⁺ CD21⁺ CD23⁺ IgM⁺ IgD⁻ by flow cytometry.

Figure 3. Hypergammaglobulinemia, bone marrow plasmacytic infiltration, and X-ray analysis of the bones in *Eμ c-Maf* transgenic mice. A, Representative results of electrophoresis of the serum proteins. Note the presence of an M spike (arrow) in *Eμ c-Maf* transgenic mice at 50 weeks old. B, Marked elevation of serum immunoglobulin levels in *Eμ c-Maf* transgenic mice. Sera from *wild-type* (○; n=7) and *Eμ c-Maf* transgenic (●; n=14) mice at 50 weeks old were analyzed by ELISA (upper panel). The plot shows both IgG and IgM levels in *Eμ c-Maf* transgenic mice at 50 weeks old. Only one out of the 14 mice showed high levels of both IgG and IgM (lower panel). C, Representative bone marrow biopsies from *wild-type* (WT) and *Eμ c-Maf* transgenic (TG) mice were analyzed by light microscopy (H&E) to reveal increased plasma cell infiltrates in the marrow of *Eμ c-Maf* transgenic mice. FACS analysis also revealed that the numbers of mature plasma cells (B220^{low} CD138⁺) and B220⁺ CD138⁺ cells were increased in the bone marrow in the transgenic mice. Obvious osteolytic lesions could not be found in 50 weeks old *Eμ c-Maf* transgenic mice by X-ray analysis.

Figure 4. Renal involvement in *Eμ c-Maf* transgenic mice. A, Renal tissue sections from 60 weeks old *Eμ c-Maf* transgenic (TG) mice with lymphoma and *wild-type* (WT)

mice were stained with PAS. Left panels show renal tubules, whereas right panels represent glomeruli. B, Glomerular immunoglobulin deposition. Serial frozen sections of renal tissue from *wild-type* and *E μ c-Maf* transgenic mice were analyzed by immunofluorescent staining using specific antibodies against mouse immunoglobulin kappa and lambda light chains, as well as antibodies against IgG, IgM, and IgA heavy chains..

Figure 5. Autonomous proliferation of c-Maf-induced lymphoma cells. A, Mononuclear cells that had been isolated from the spleens of *E μ c-Maf* transgenic mice and transplanted into nude mice infiltrated the spleens of the recipient mice. Enlarged liver and spleen were observed in the recipient mouse. B, Southern blot analyses of lymphoma cells from the spleens of *E μ c-Maf* transgenic mice using a *JH4* probe after digestion with *EcoR* I. Lane 1 (DNA from tail of a *wild-type* mouse), lane 2 (DNA from the tail of an *E μ c-Maf* transgenic mouse), and lanes 3 to 6 (DNA from the enlarged spleens from *E μ c-Maf* transgenic mice) show the presence of a DNA fragment corresponding to the germ line *JH4* gene (solid arrow). Lanes 3 to 6 show DNA fragments that corresponded to rearrangements of the *IgH* gene (asterisk). Lanes 2 to 6 show a DNA fragment that corresponded to the *IgH* transgene (hollow arrow). C, Transplanted tumor cells showed a plasma cell-like appearance in the spleens of the recipients, as shown by H&E staining.

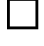

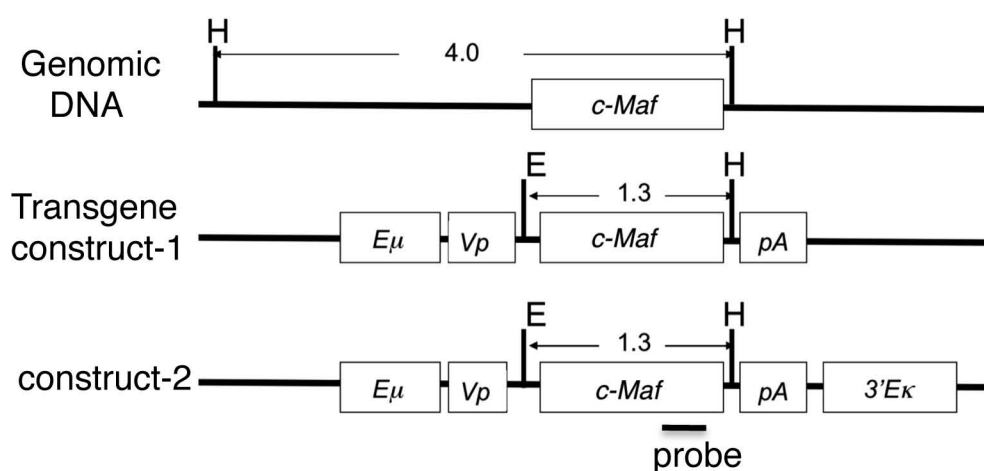
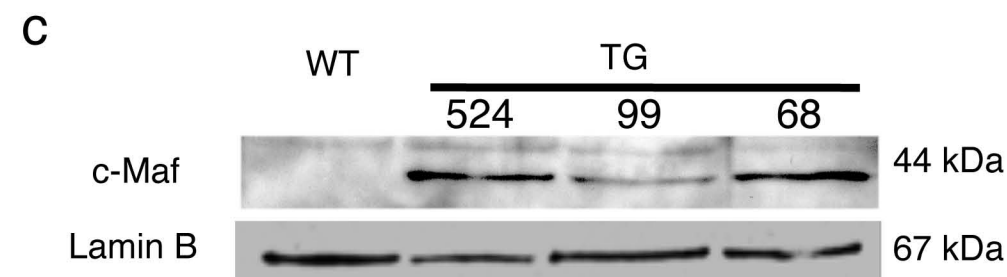
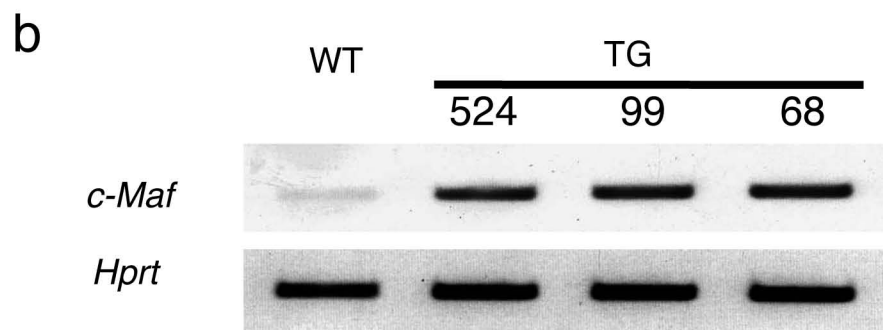
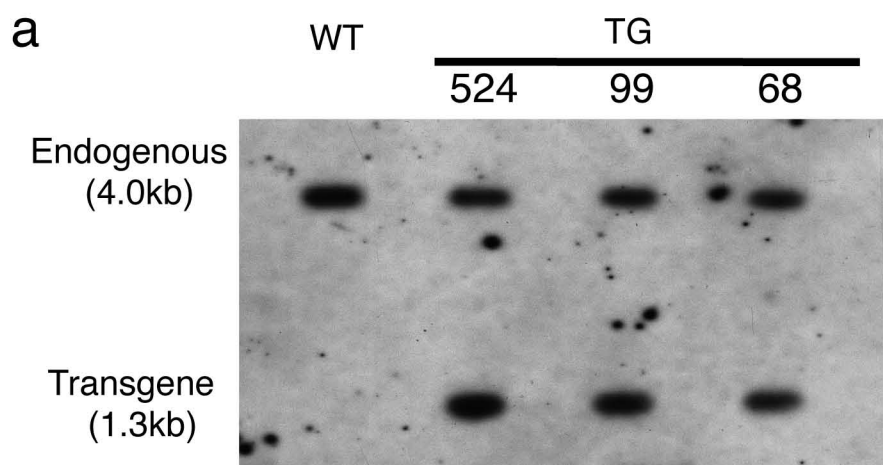
Figure 6. Analysis of *c-Maf* target genes by quantitative RT-PCR. The expression profiles of *Maf* (*c-Maf*) and its target genes were examined by real-time RT-PCR analysis. Total RNA was obtained from the enlarged lymph nodes from *Eμ c-Maf* transgenic mice. All of the data are presented as the mean \pm SE. , WT; mRNA from B220⁺ B cells from the spleens of 50 weeks old *wild-type* mice, , TG; mRNA from the lymph nodes of mice from *Eμ c-Maf* TG line 524. * indicates $p < 0.05$.

Figure 1

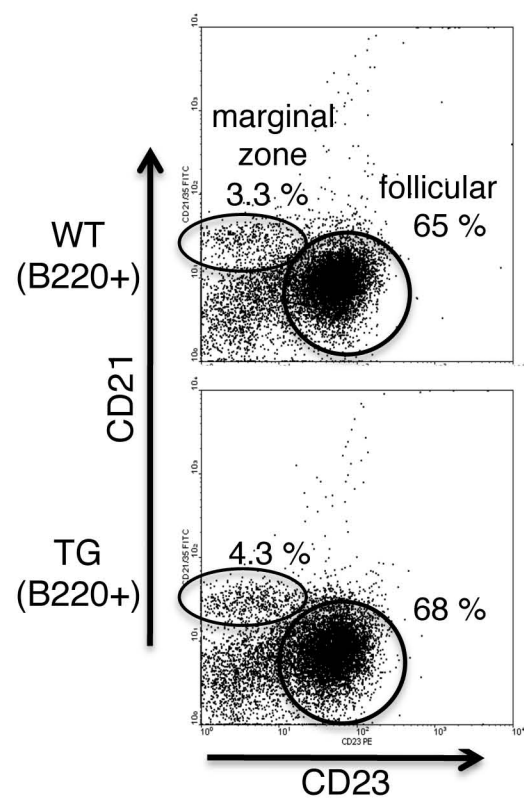
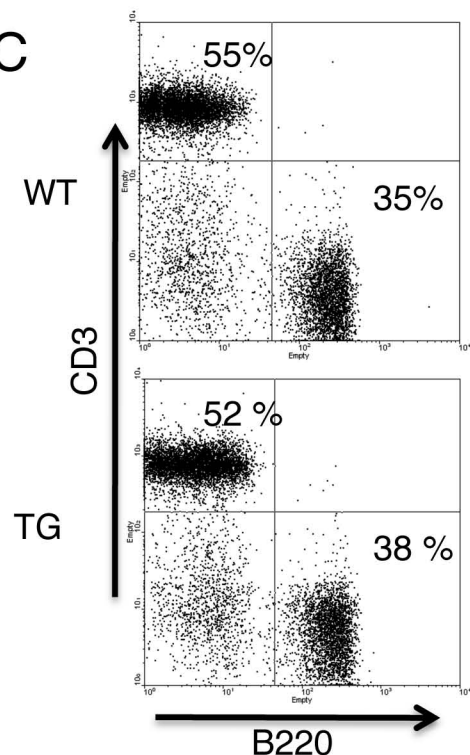
A



B



C



D

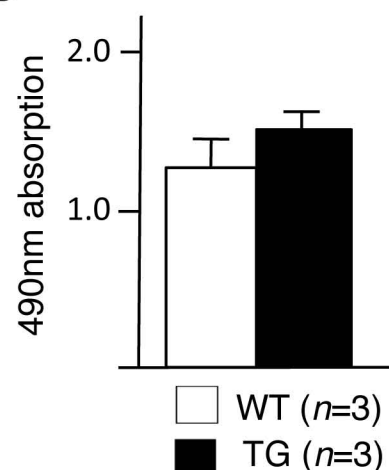


Figure 2

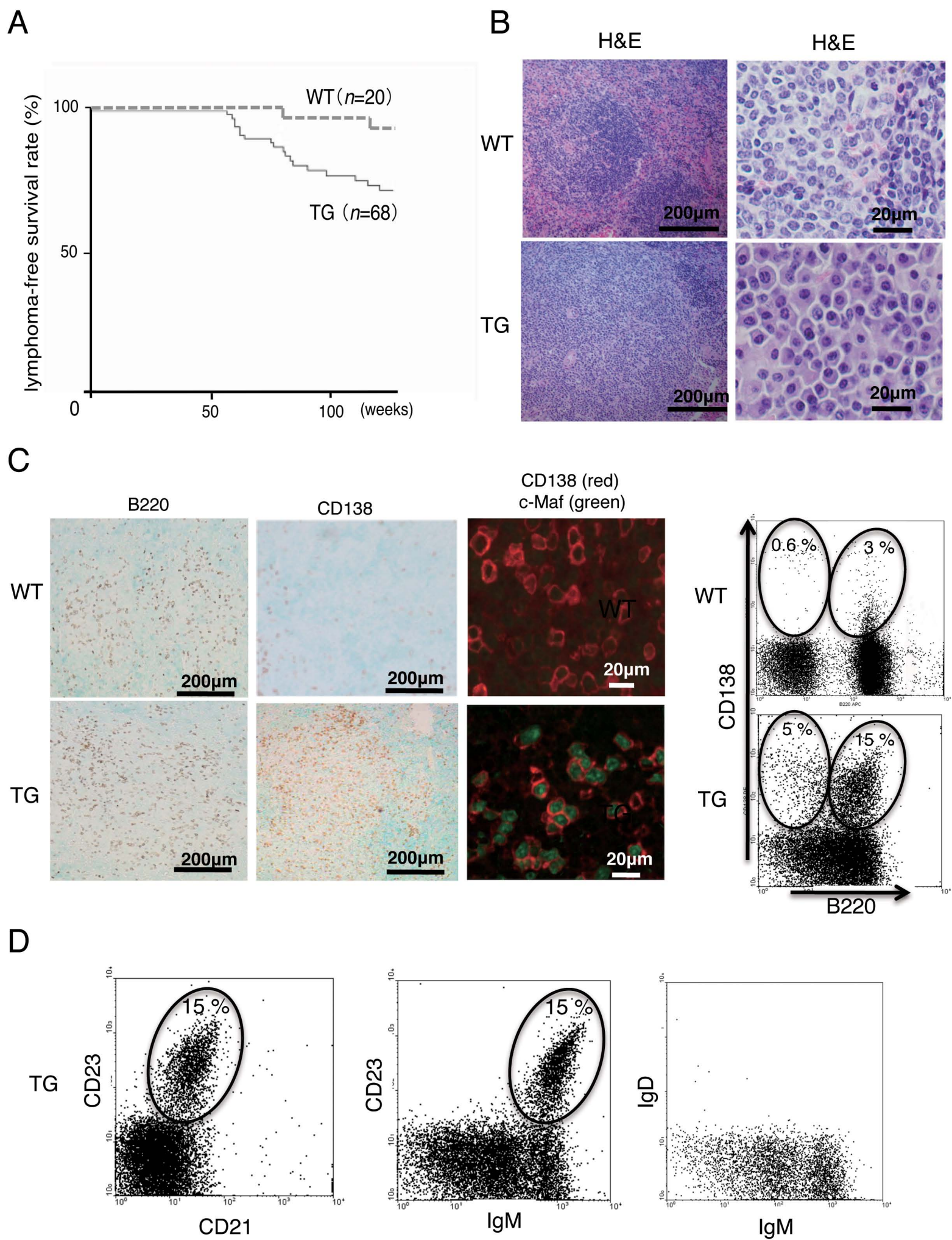
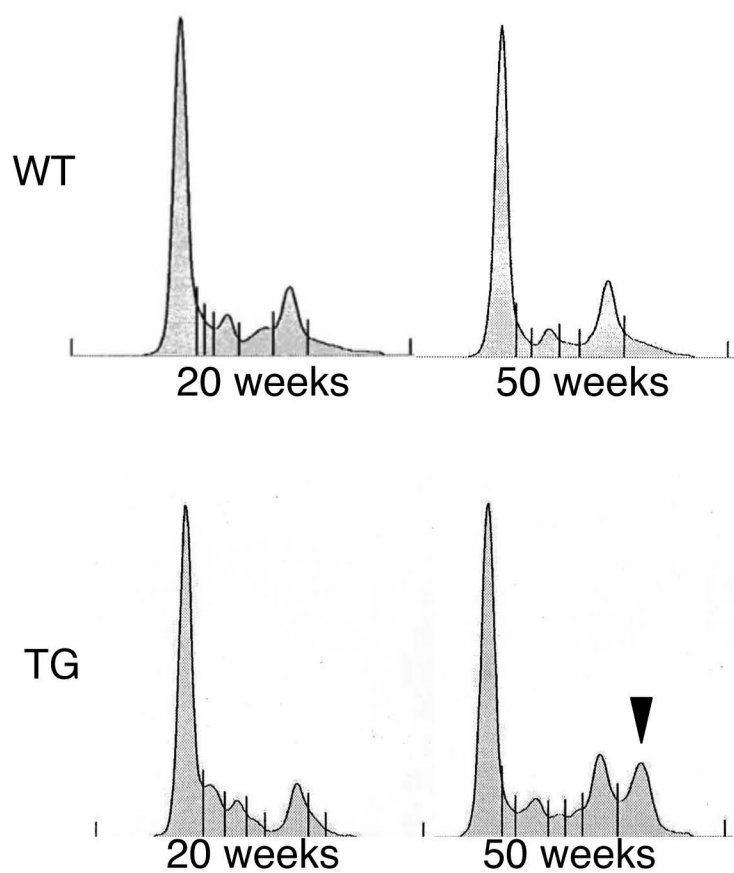
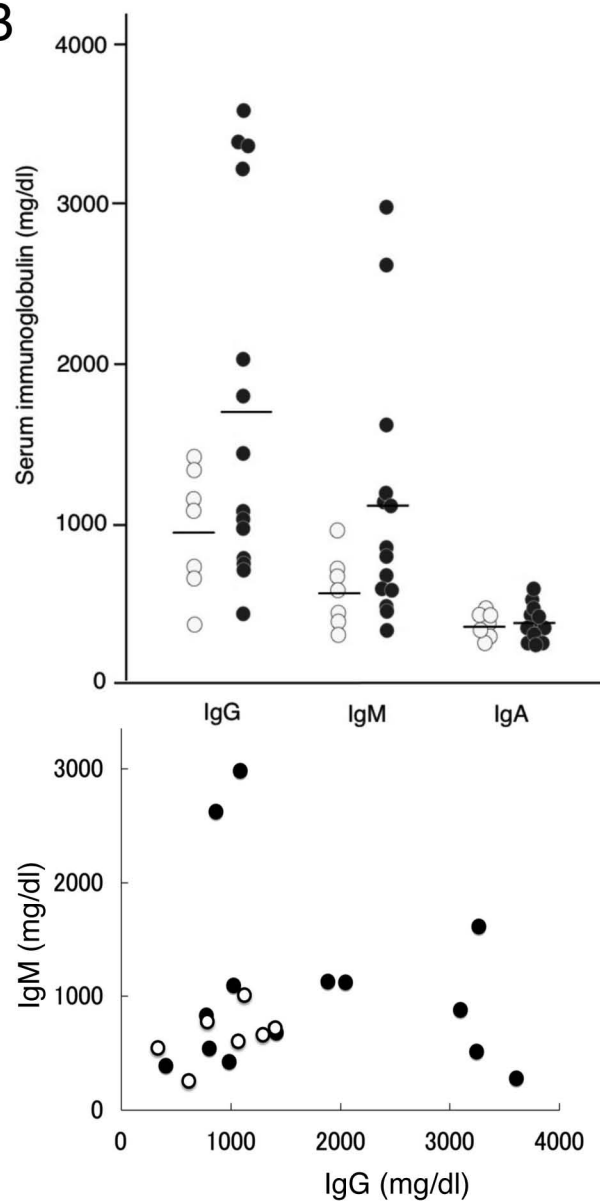


Figure 3

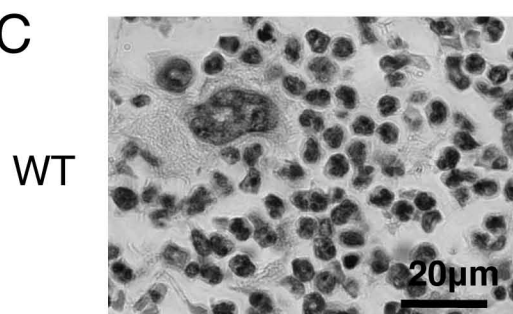
A



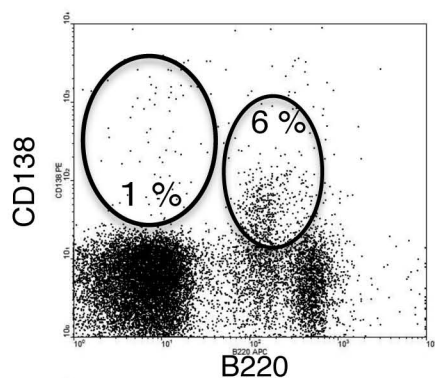
B



C



WT



TG

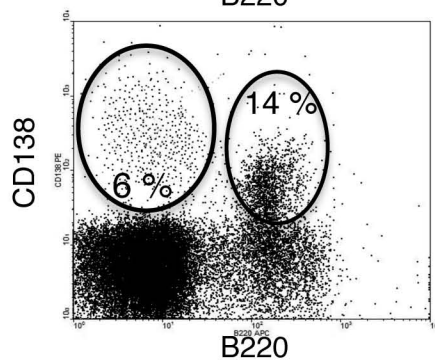
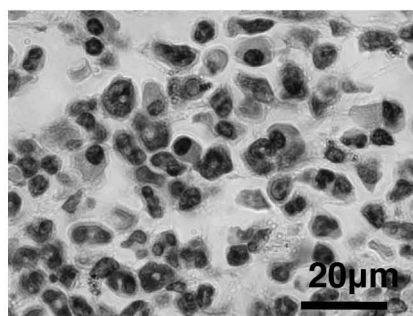


Figure 4

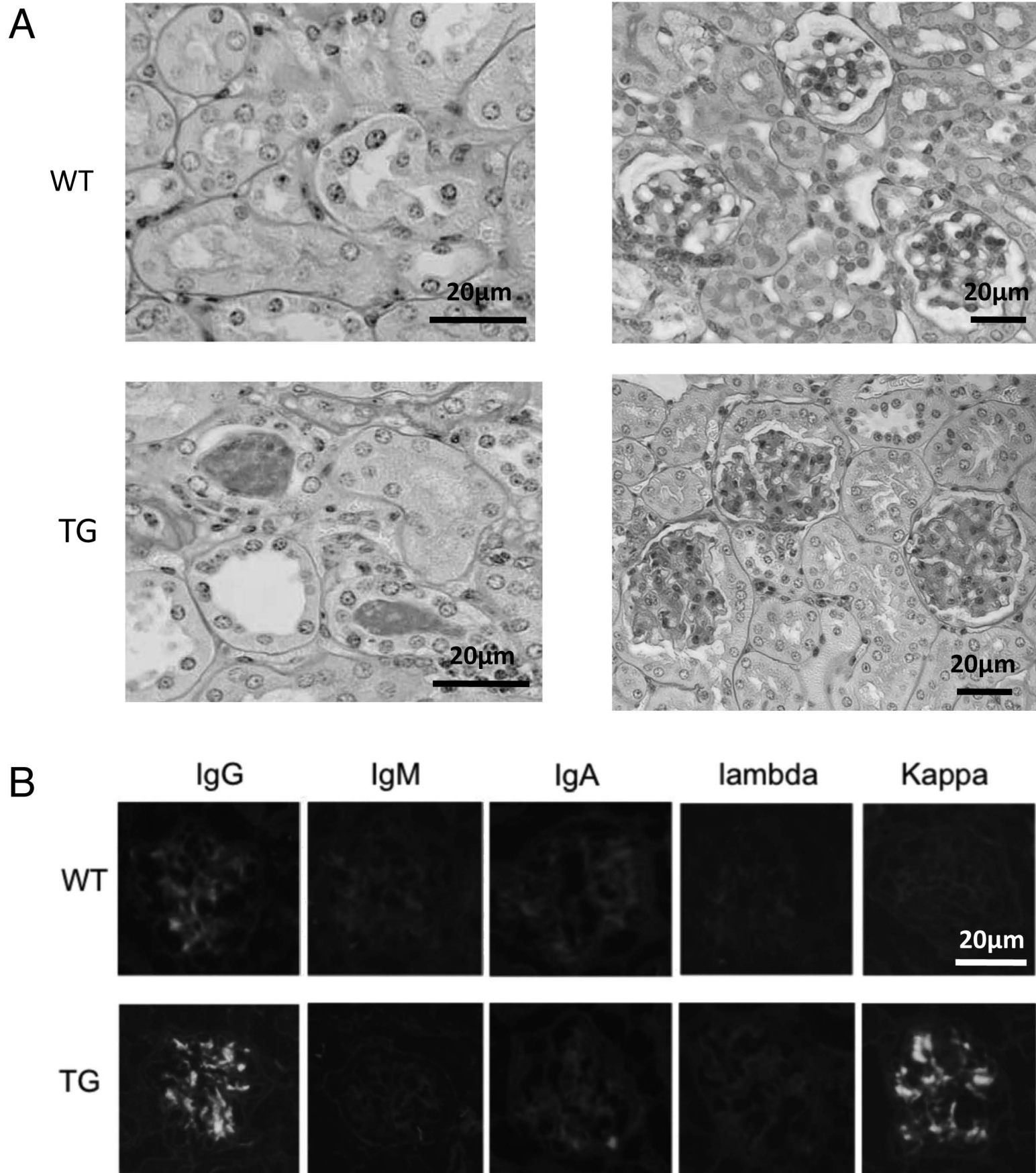


Figure 5

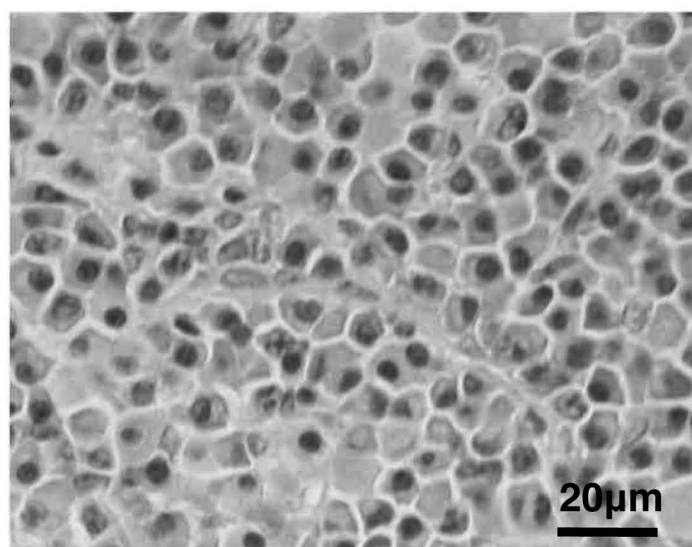
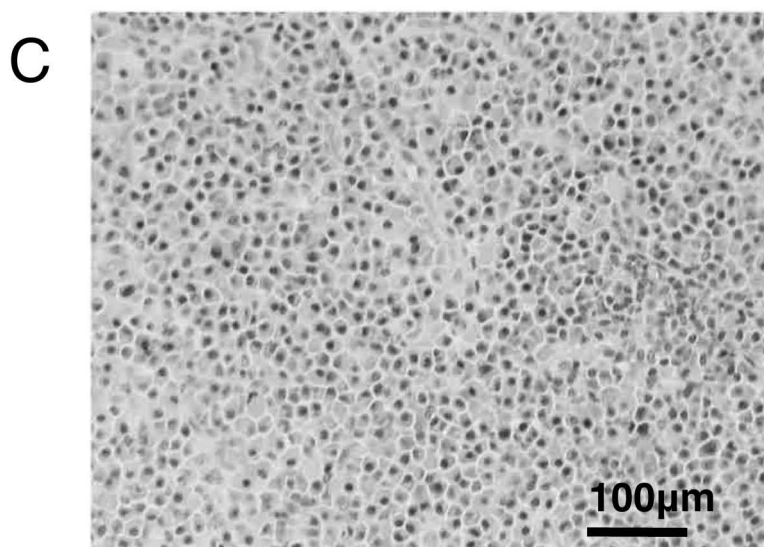
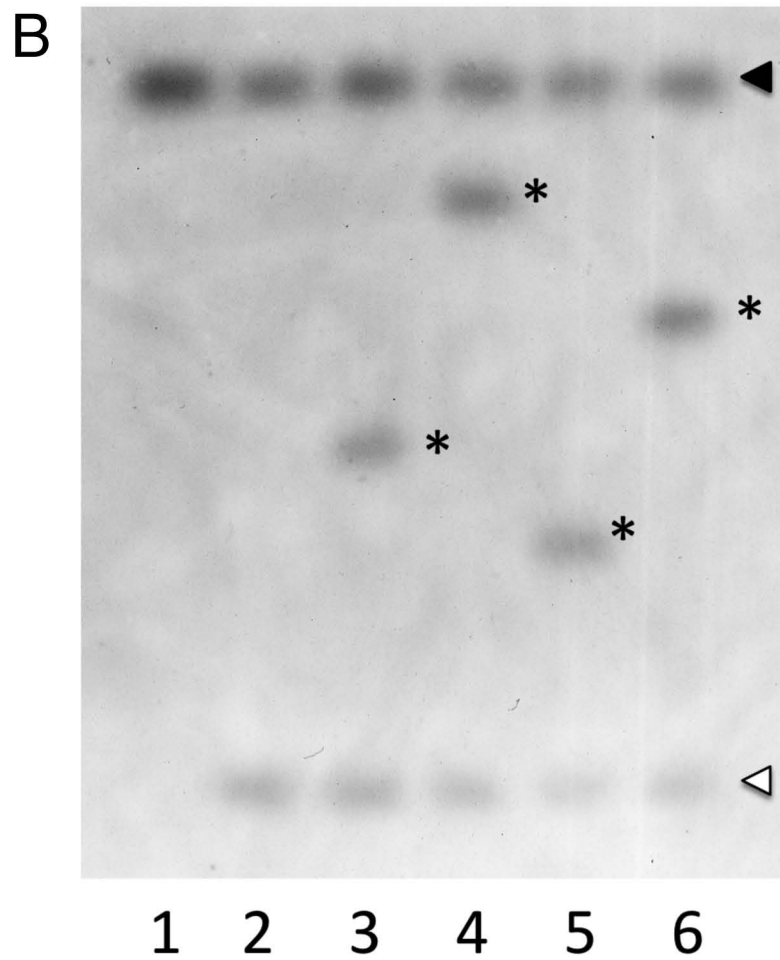
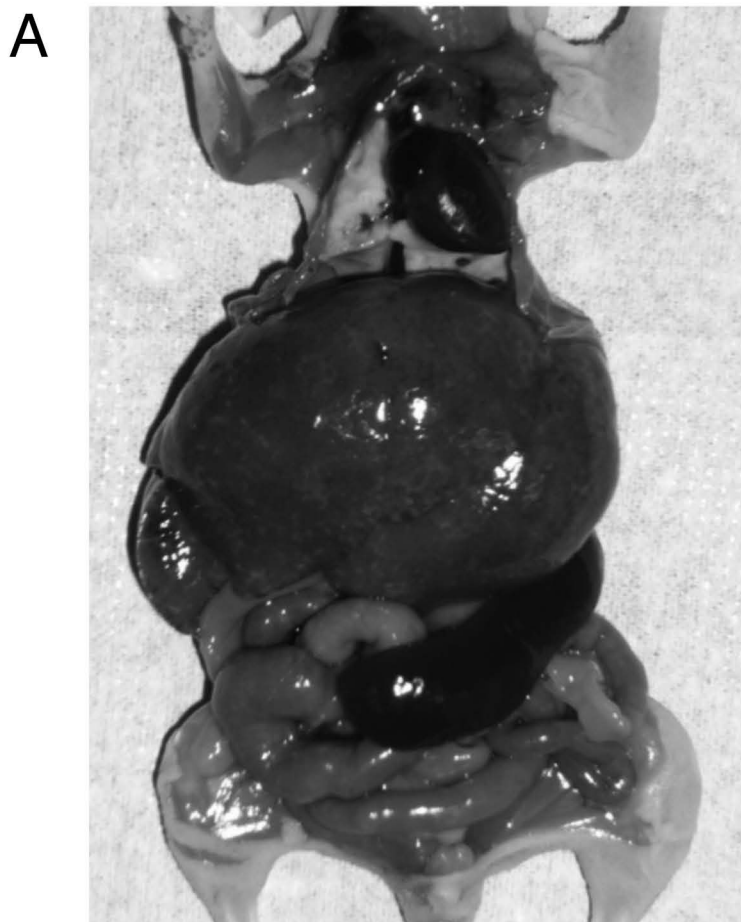


Figure 6

